Final report for the period April 1995 - September 2002
ONR
Grant N00014-95-1-054
Program Officers: Thomas Kinder, Linwood Vincent and Thomas Drake

The Dynamics of Cobbles in and Near the Surf Zone

Don L. Boyer, P.I.

Harindra J.S. Fernando, Co-P.I.

Sergey I. Voropayev, Co-P.I.

Arizona State University

Department of Mechanical and Aerospace Engineering

Tempe, AZ 85287-6106

phone: (480) 965-1382, fax: (480) 965-1384, e-mail: don.boyer@asu.edu

http://www.eas.asu.edu/~pefdhome

REPORT DOCUMENTATION PAGE

Form Approved
OMB No. 0704-0188

1. REPORT DATE *(DD-MM-YYYY)*	2. REPORT TYPE	3. DATES COVERED *(From - To)*
20/02/03	FINAL TECHNICAL REPORT	4/1/95 - 9/30/02

4. TITLE AND SUBTITLE
The Dynamics of Cobbles in and Near the Surf Zone

5a. CONTRACT NUMBER

5b. GRANT NUMBER
N00014-95-1-0543

5c. PROGRAM ELEMENT NUMBER

6. AUTHOR(S)
Don L. Boyer ; Harindra J.S. Fernando; Sergey I. Voropayev

5d. PROJECT NUMBER

5e. TASK NUMBER

5f. WORK UNIT NUMBER

7. PERFORMING ORGANIZATION NAME(S) AND ADDRESS(ES)

Arizona State University
Dept. of Mechanical and
Aerospace Engineering
Tempe, AZ 85287-6106

8. PERFORMING ORGANIZATION REPORT NUMBER

XAA 1879/TE

9. SPONSORING / MONITORING AGENCY NAME(S) AND ADDRESS(ES)

Office of Naval Research
Ballston Centre Tower One
800 North Quincy Street
Arlington, VA 22217-5660

C.L. Vincent, T. Drake
ONR 321CD

10. SPONSOR/MONITOR'S ACRONYM(S)
ONR

11. SPONSOR/MONITOR'S REPORT NUMBER(S)

12. DISTRIBUTION / AVAILABILITY STATEMENT

Approved for Public Release; distribution is Unlimited.

13. SUPPLEMENTARY NOTES

14. ABSTRACT

This research was driven by the need of the Navy to improve mine countermeasures in support of joint littoral warfare, for which a ke paradigm is to locate a clear or low mine- and obstacle-density path. To accomplish this goal, it is imperative that one be able to predict th behavior of mines in shallow water under a variety of coastal-ocean conditions. A laboratory experimental program, coupled with theoretica modeling, was conducted at Arizona State University for the purpose of improving scientific understanding and predictive capabilities of th dynamics of the motion and scour/burial of cobbles/mines within very shallow water in and near the surf zone. Results of these studies ar summarized in this report. To model the oscillatory water motion in different regions of the surf zone, three experimental installations wer constructed and used: (i) dam break tank for flow in a swash region, (ii) standing wave tank for oscillatory flow near the surf and (iii) larg wave tank to model flow in the entire surf zone, including wave breaking region. The data on the motion of cobbles/mines along solid bottor at different flow conditions were collected and the results were explained theoretically. In the case of a sandy bed, detailed data on th bottom morphodynamics (sand ripples and bars formation and evolution) were collected and explained theoretically. Different scenarios c cobble/mine behavior on a sandy bed were simulated experimentally and explained theoretically. These include: (i) slow, mostly onshore drift of cobbles, (ii) scour around cobbles, (iii) periodic burial under drifting ripples, and (iv) permanent burial under migrating sand bars.

15. SUBJECT TERMS

16. SECURITY CLASSIFICATION OF:			17. LIMITATION OF ABSTRACT	18. NUMBER OF PAGES	19a. NAME OF RESPONSIBLE PERSON
a. REPORT	b. ABSTRACT	c. THIS PAGE			Harindra J.S. Fernando
					19b. TELEPHONE NUMBER *(include area code)* (480) 965-2807

Table of Contents

Abstract

This research was driven by the need of the Navy to improve mine countermeasures in support of joint littoral warfare, for which a key paradigm is to locate a clear or low mine- and obstacle-density path. To accomplish this goal, it is imperative that one be able to predict the behavior of mines in shallow water under a variety of coastal-ocean conditions. A laboratory experimental program, coupled with theoretical modeling, was conducted at Arizona State University for the purpose of improving scientific understanding and predictive capabilities of the dynamics of the motion and scour/burial of cobbles/mines within very shallow water in and near the surf zone. Results of these studies are summarized in this report.

To model the oscillatory water motion in different regions of the surf zone, three experimental installations were constructed and used: (i) dam break tank for flow in a swash region, (ii) standing wave tank for oscillatory flow near the surf and (iii) large wave tank to model flow in the entire surf zone, including wave breaking region. The data on the motion of cobbles/mines along solid bottom at different flow conditions were collected and the results were explained theoretically. In the case of a sandy bed, detailed data on the bottom morphodynamics (sand ripples and bars formation and evolution) were collected and explained theoretically. Different scenarios of cobble/mine behavior on a sandy bed were simulated experimentally and explained theoretically. These include: (i) slow, mostly onshore, drift of cobbles, (ii) scour around cobbles, (iii) periodic burial under drifting ripples, and (iv) permanent burial under migrating sand bars.

1. Introduction

During the past several years, the Office of Naval Research (ONR) has supported a research program at Arizona State University (ASU) aimed at understanding the dynamics of large bottom particles (cobbles/mines) subjected to periodic background flows akin to those found along the sea floor in coastal environments. This problem has important applications to mine countermeasure efforts of the U.S. Navy in littoral zone. Following the Gulf War (Desert Storm), the U.S. naval strategy has been increasingly focused on littoral warfare, with major emphases on operational and naval fleet aids in coastal environments. Providing tactical support in such environments requires reliable predictive capabilities of the fate and distribution of mines, which can be accomplished using probabilistic models of mine behavior. Development of these models requires a fundamental understanding of the physics and dynamics of flow-mine-sand interactions, and this understanding at the time of initiation of our research was insufficient.

Taking this into account, a comprehensive research program was directed primarily to understanding the (i) dynamics of cobbles/mines on solid bed with artificial roughness, (ii) morphodynamics of sandy bed, and (iii) cobbles/mines scour/burial mechanisms on a sandy bed. Parameterization of theses processes in conditions similar to those that occur in and near the surf zone was also of interest. The focus was primarily on smaller cobbles/mines in the shallow surf zone (e.g., anti-tank mines), rather than large "non-walking" anti-ship mines in deeper coastal waters, the latter being the theme of the ONR Mine Burial Program. These efforts paralleled the objectives of the Organic Mine Countermeasures (OMCM) Future Naval Capabilities (FNC) program of the Office of Naval Research.

Over the years, extensive research has been conducted on the dynamics of wave motion in and near the surf zone (see the schematic in Fig. 1) and on the resulting sediment transport (Louguet-Higgins & Stewart, 1964; Yalin, 1977; Engelund & Fredsoe, 1982; Peregrina, 1983; Sleath, 1984; Craik, 1985; Battjes, 1988; Mei, 1982, 1985, Mei & Liu, 1993; Mei & Yu, 1997; Fredsoe & Deigaard, 1992; Nielsen, 1992; Belorgey et al., 1993; Arcilla et al., 1994; Dean & Dalrymple, 1994; Yu & Mei, 2000; Ridler & Sleath, 2000). Most of these studies have concentrated on fine sediment transport, but only little attention has been given to much larger sediment particles of the size of cobbles. (Cobbles are defined by the American Geophysical Union as sediment particles with typical diameter D = 6.4 - 25.6 cm; Sleath, 1984). Besides

obvious engineering and geophysical applications, the transport of such large particles is a topic of current interest to the Navy, given that their behavior has similarities to that of anti-tank mines placed in coastal waters (Lott & Poeckert, 1996).

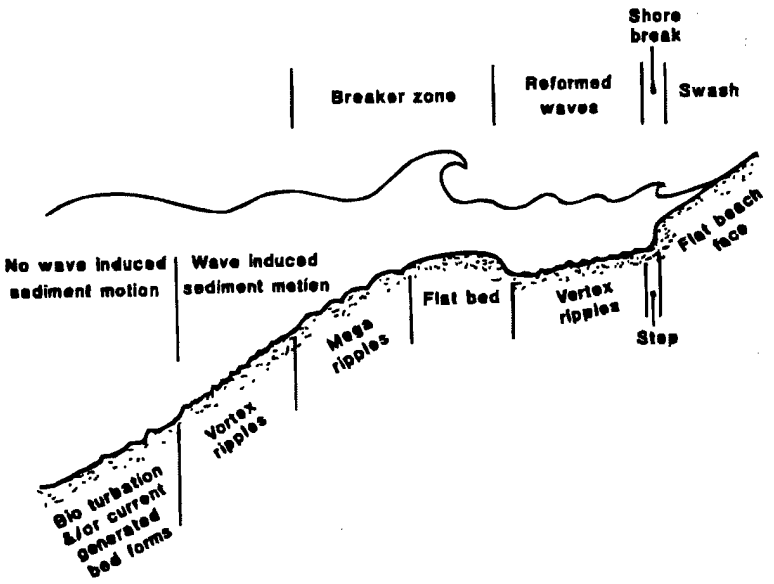

Figure. 1. *Schematic showing different regions of the surf zone (Nielsen, 1992).*

Motivated by the important naval problem of being able to predict the behavior and fate of relatively small land mines in and near the surf zone, a research program supported by the Coastal Dynamics Program of the ONR was initiated at ASU. In contrast to the rather extensive literature that exists on the transport of fine sediments in the coastal region, prior to the said program at ASU, very little research had been done on the behavior of cobbles/mines on sloping sandy beaches. During the period of this grant, the ASU group made steady progress in developing a better understanding of cobble/mine behavior and their burial as driven by the surf.

The long-range goals of this research were to develop, using laboratory experiments, theoretical and, in some cases, numerical analyses, a basic understanding and, eventually, a predictive capability, of the behavior of cobbles/mines in the shoaling, wave-breaking and swash regions. Disk-shaped anti-tank mines are of comparable size and density.

The scientific objectives of our research were directed toward better understanding the behavior of cobbles on beaches, which are permeable with movable sand bedforms. These

objectives permited a better understanding of (i) the long-time dynamics of bottom topography (morphodynamics) including sand ripples and bars formed in a model surf zone, and (ii) the processes related to scour and periodic/permanent burial of cobbles on a sandy beach with ripples and bars in time- and space-dependent surf-zone flow. In particular, we studied (i) the evolution of an initially flat sandy beach; (ii) the long-time behavior of the bottom topography, and (iii) the behavior of model cobbles on solid and sandy beds

The approach in this research was mostly experimental. Considering the nascent nature of research on this problem, a step-by-step approach from simplified and idealized situations to more realistic, and subsequently much more complicated configurations, was adopted. Realizing that carefully designed experiments are an avenue for achieving the scientific goals, a number of experimental facilities for cobble/mine research were designed and developed at Arizona State University. These include: (i) three different experimental facilities capable of reproducing different basic background flows that occur in and near the surf zone; (ii) a system of devices to control and measure the mean and turbulent flow characteristics and other parameters; and (iii) instrumentation for employing different methods of flow visualization (see Section 2 below).

The initial studies focused on cobble/mine motion along impermeable beaches. At first, a series of experiments was conducted in which the dynamics of cobbles/mines placed on a solid slope with artificial roughness was studied in background flows similar to those observed in different regions of the surf zone. Large standing waves and turbulent bores were used to model, respectively, steady oscillations and swash flows (Luccio et al., 1998; Voropayev et al., 1998). A layer of sand was then introduced at the bottom of the water tank and the dynamics of sand ripples and behavior of cobbles/mines were studied under oscillatory flow conditions (Voropayev et al., 1999). This work acted as a precursor to the studies of cobble/mine scour/burial on sloping sandy beaches.

The presence of sand significantly complicates the problem. When the fluid velocity exceeds some critical value, ripples are formed on an initially flat sandy bed, which affect the behavior and burial/scouring of cobbles. Although the physical mechanism of ripple formation is qualitatively well understood (see Horikawa & Wanatabe, 1967, Sleath, 1976; 1984, 1995 and references therein), owing to the complexity of the problem a quantitative theory in this regard was still in infancy. In particular, linear and weakly nonlinear analyses have been conducted only recently (Blondeaux, 1990; Vittory & Blondeaux, 1990; Blondeaux et al., 2000) for the case

of small rolling-grain ripples. These are observed at small velocities of fluid oscillations. At larger velocities the height of the rolling-grain ripples increases and flow separation occurs. As a result, relatively large so-called vortex ripples are formed (Fig. 2).

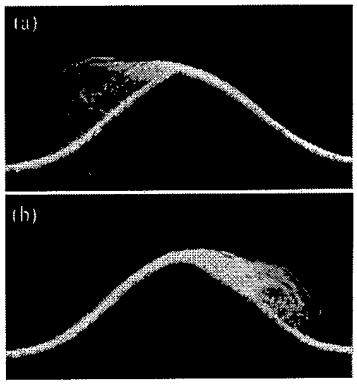

Figure 2. *Large vortices shed periodically from symmetric sand ripples that are formed in symmetric oscillatory flow induced by standing waves. The water moves (a) from right to left and (b) from left to right (Voropayev et al. 1999).*

Analytical theories for such complicated nonlinear flows remain untenable; empirical and semi-empirical models of varying complexities, however, are in frequent use (Sleath, 1984, 1995; Nielsen, 1992). Needless to say, the presence of a movable sandy bed and its time evolution extensively modify the behavior of cobbles/mines. Our experiments (Voropayev et al., 1999) show that, owing to large-time instabilities, the bed shape does not reach a steady state. The ripples migrate with time and their migration leads to periodic burial/scouring of cobbles.

More realistic modeling of typical conditions that are observed in the oceanic surf zone required large-scale experiments. Supported by ONR, a large wave tank with a slope was constructed at ASU. A series of experiments was conducted and theoretical models for cobble/mine behavior, which were developed and tested previously for simplified flow configurations, were tested and improved for surf conditions with a solid bottom (Voropayev et al., 2001). Surf conditions with a sandy slope were then considered (Voropayev et al., 2000, 2003). Based on the results of these experiments, a physical understanding of a wide range of phenomena was attained and theoretical models describing them were developed and tested. The principal results of these studies are reported in our publications (which are given at the end of this report) and summarized in the next sections.

2. Experimental installations and flow characteristics

Mostly disc-shaped cobbles/mines were used in the experiments, but in some cases spherical objects were also used. Because the spherical cobbles may roll, their moment of inertia becomes an important parameter and to change its value in selected experiments spherical shells filled with different liquids were also used. In total more than 20 different cobbles were used in experiments. Typical disc-shaped cobbles used in experiments conducted in a large wave tank are shown in Fig. 3, and some of their characteristics are given in Table 1 (diameter D, height h_C, density ρ_C and static K_S and dynamic K friction coefficients). Both K_S and K were estimated by dragging with relatively small velocity the submerged cobbles along the tank floor, and measuring the force for initiation of motion and force in a steady motion by a standard sensitive electronic scale. The static friction coefficient was up to two times higher than the dynamic friction coefficient (see Table 1). This means that the force one must apply to initiate the motion is twice as large as the force one must exert to keep it moving.

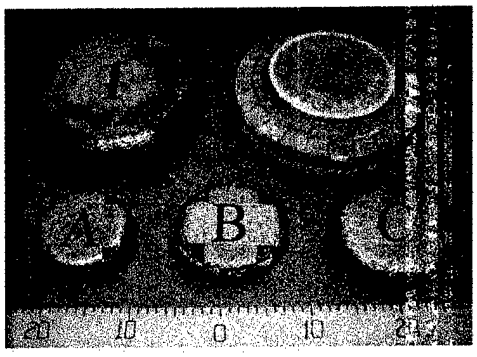

Figure 3. *Model cobbles/mines used in the experiments. Scale is in cm. Other parameters are given in Table 1.*

Table 1

	D (cm)	h (cm)	ρ_C (gcm^{-3})	K	K_S
1	19.5	8.5	1.21	0.5	0.8
2	21.7	9.1	119	0.3	0.5
A	10.3	5.3	1.18	0.5	0.8
B	11.7	4.7	114	0.5	0.8
C	13.0	5.4	1.11	0.5	0.8

To model flows in different regions of a surf zone, three different experimental installations were constructed and used in these studies.

Swash flow. In the first installation a dam break flow was used to model flow in a swash region (Fig. 4). In this approach, a dam or gate, which, prior to the experiment, blocks a

reservoir of water, is nearly instantaneously removed. This results in a well-defined and reproducible bore which moves through the uniform channel of rectangular cross-section. By varying the height H_0 of the water behind the dam, the height and propagation speed of the bore can be varied (Fig. 5).

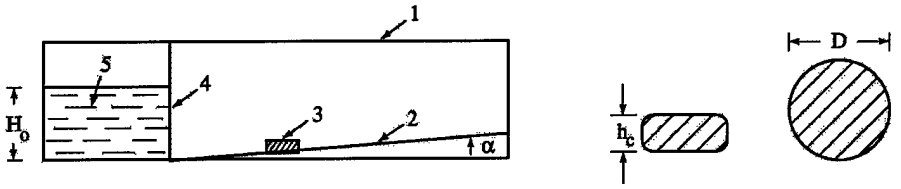

Figure 4. *Schematic diagram of (a) the experimental dam break flow set-up and (b) model cobble; 1-tank, 2-sloping bottom, 3-cobble, 4-gate, 5-water.*

Two similarities can be noted between a breaking wave impinging on a beach and a turbulent bore; i.e., shape and speed. Apart from these large-scale visual similarities, there is also an internal dynamical similarity; namely, the energy lost through the dissipation in a bore gives realistic estimates of the energy lost in the surf zone (e.g., see Fredsoe & Deigaard, 1992). These similarities are the principal reasons the dam-break method was chosen to model the water motion in a swash zone.

Figure 5. *Dam-break flow: Solid line - water surface without friction, dashed line - correction for bottom friction at the tip of the front.*

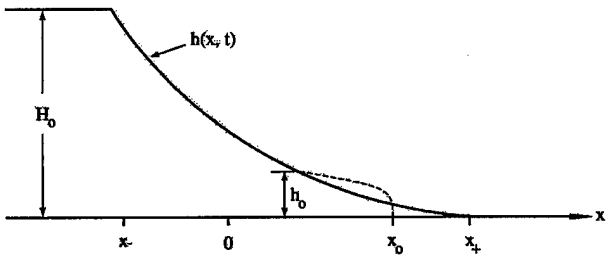

The great advantage of this method is that the background velocity produced by the dam break flow is reasonably well analyzed theoretically (Whitham, 1955, 1974) and to a good approximation can be parameterized as

$$u = a_1(gH_0)^{1/2}$$

(a_1 = const ≈ 2/3, see details in Luccio et al., 1998).

In the experiments the cobbles were placed at a fixed distance from the gate along the tank axis (Fig. 6a). The gate was opened and the water front was created. The distance from the gate to the initial position of the cobble was the same (50 cm) in all runs. This distance was chosen empirically in order to provide a tip of approximately constant height as the water front reached the cobble. Upon impingement of the water front, (Fig. 6b), the cobble started to move (Fig. 6c) with a velocity $U = dx_c/dt$, where x_c is the cobble displacement from the initial position at t = 0.

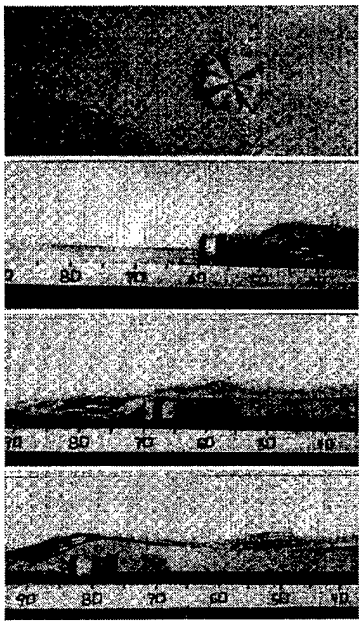

Figure 6. *The motion of a cobble in a dam-break flow: (a) - top view, (b-c) - side view; (a) - t < 0, (b) - t = 0, (c) - t = 0.04 s, (d) - t = 0.67 s. The flow moves from right to left. The time origin, t = 0, is chosen at the moment when cobble, which was initially at rest at x = 50 cm, starts to move. Experimental conditions: H_0 = 20 cm, D = 10 cm, h_C = 4 cm, ρ_C = 1.5 gm cm^{-3}.*

Two separate tank floors were used in the experiments; i.e., smooth (Plexiglas) and rough, for which a thin layer of sand was glued to the Plexiglas. This permitted a variation of the kinetic friction coefficient K between the bottom and cobble by a factor of four. By tilting the bottom at a small angle to the horizontal, the effect of a sloping bottom was modeled in the experiments. A total more than 40 experiments were conducted with different initial conditions and data on the cobble displacements as a function of time were taken using a video camera with high resolution.

Oscillatory flow was modeled using standing waves induced in a large (length L = 366 cm) tank of rectangular cross-section (Fig. 7). The waves were forced by a vertical paddle installed at one end of the tank and connected through a mechanical drive to a precision motor;

the paddle oscillates with a prescribed amplitude and frequency, ω, thus generating periodic progressive surface waves of the amplitude a/2. When these waves reach the end wall of the tank, they reflect without a significant loss of amplitude and propagate in the opposite direction with the same frequency. The superposition of these progressive waves leads to a standing wave pattern. The vertical velocity near the central portion of the tank is small, while the horizontal velocity u is practically depth independent and can be approximated as (Whitham, 1974)

$$u \approx \varepsilon\omega \sin\frac{\pi x}{L}\sin\omega t \approx \varepsilon\omega \sin\omega t,$$

where $\varepsilon = aL/(\pi h_0)$ (h_0 is the water depth). Employing standing waves of the first mode, it was possible to produce horizontal oscillations in the central potion of the tank with velocity amplitude up to 80 cms^{-1}.

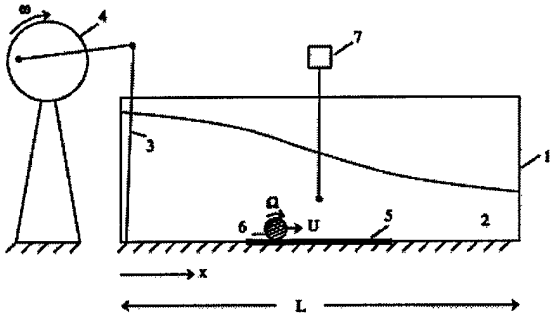

Figure. 7. *Standing wave tank: 1 - tank, 2 - water, 3 - paddle, 4 - eccentric drive mechanism, 5 – solid bottom with artificial roughness or layer of sand, 6 - cobble, 7 - ADV probe.*

In the experiments, a cobble was placed on the floor in the vicinity of the tank center and its subsequent motion was investigated. Two different cobble shapes were considered; i.e, spheres of diameter D and density ρ_C and disks of diameter D, height h_C and density ρ_C. Typical parameter values used were D = 1.2-22 cm, h_C= 2-5 cm, ρ_C = 1.04-7.9 gcm^{-3} (for details see Voropayev et al., 1998). The central portion of the tank floor was removable and was either smooth or rough (sand-covered plate). This allowed a variation of the coefficient of friction between the cobble and the floor in a factor of 5.

The model cobble (sphere or disk) was placed on the solid floor near the center of the tank and its position (and the angular velocity for spherical cobbles) was monitored. Then a layer of sand (depth 15 cm) was placed at the bottom. In these experiments the time evolution of the sandy bed (without cobbles) was studied and data on the formation and drift of vortex ripples were collected. Then selected cobbles were placed at sandy bed and their behavior (motion,

scour/burial) was studied. In total more than 80 experiments were conducted using this standing wave tank

A large wave tank was used to model the water motion in the entire surf zone, which includes shoaling, wave-breaking and swash regions. This glass-walled wave tank (length 32 m, width 0.9 m, depth 1.8 m) was designed and constructed at ASU. An oblique view of the tank is given in Fig. 8 and the schematic of the experimental system is shown in Fig. 9. The plane vertical paddle, installed at one end of the tank and driving by a piston, is used to generate periodic waves. The wave maker is driven by a hydraulic system, which is capable of producing a periodic sinusoidal or step-like motion with a highly stable frequency. Periodic sinusoidal waves of frequency ω = 0.2-0.7 Hz and peak-to-peak amplitude of the paddle motion up to 2ε = 25 cm were used in most of the experiments. A wooden bottom with slope 1:24 (length 26 m) is installed opposite to the paddle. In experiments with solid bottom a thin layer of sand is glued on top of the sloping bottom to increase the bottom friction. In experiments with sandy bed a layer of sand (thickness 23-25 cm) was placed along the bottom.

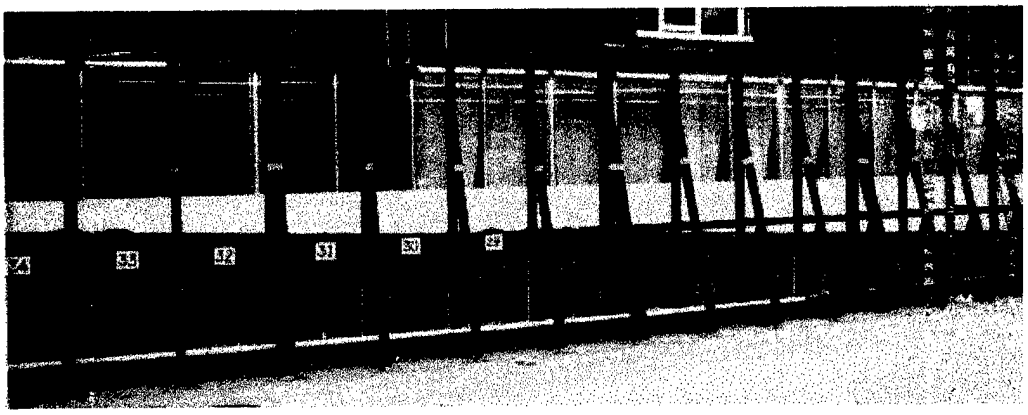

Figure 8. *The Wave tank facility that was used to model the flow in the surf zone. Numbers show the sections as counted from the wave maker, which is at the right end of the tank. The distance between vertical bars is 61 cm.*

A typical nonlinear wave propagating from right to left along sloping bottom is shown in Fig. 10. In contrast to dam break flow (Figs. 4,5) and oscillatory flow induced by large standing waves (Fig. 7), where the background flow velocity can be estimated theoretically, the flow characteristics in large wave tank cannot be estimated accurately theoretically.

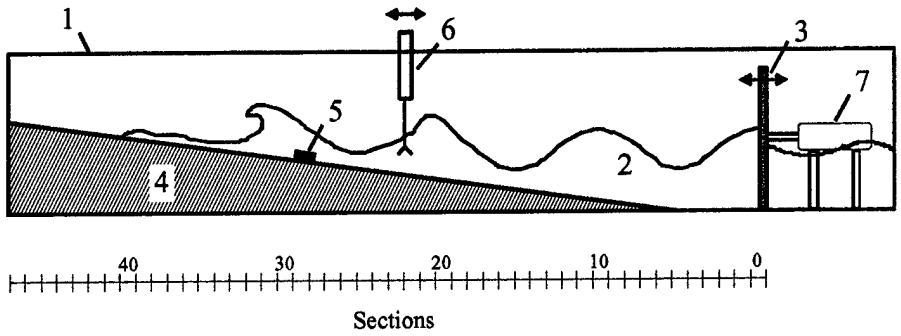

Figure 9. *Progressive wave tank experimental setup: 1 – wave tank, 2 - water, 3 – vertical wave-maker (frequency ω, amplitude of horizontal displacement ε_0), 4 – slopping solid or sand bottom, 5 – cobble, 6 – Acoustic Doppler Velocimeter (ADV) and wave gauge attached to carriage, 7 – hydraulic system to move the wave maker. Section numbers are also shown and the length of one section is 61 cm.*

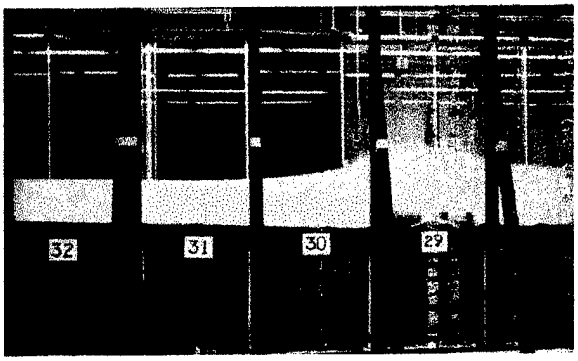

Figure 10. *A typical nonlinear wave propagating from right to left along a slope and then breaking near the break point. Two model mines are seen at the bottom in section #29.*

Significant research has been reported on weakly nonlinear waves in wave tanks (Fontanet, 1961; Madsen, 1971; Flick & Guza, 1980; Svendsen, 1985), but until now there is no satisfactory theory to accurately predict the wave characteristics and water velocities associated with strongly nonlinear shoaling waves on a slope. Although the wave-maker forcing is sinusoidal, the waves generated become increasingly nonlinear as they propagate along the slope and increase in wave steepness. In a model surf zone (Fig. 9) the background flow is a rather complicated function of time and space (see Figs. 11, 12 below), and the water particle velocities u(x,t) associated with the motion of strongly nonlinear waves (Fig. 10) propagating and breaking along the slope is rather complicated. Only recently some progress in direct numerical simulations was achieved for such flows and u(x,t) was accurately calculated but this is a rather

complicated procedure, which requires accurate preliminary calibrations (Grilli at al., 2003). As accurate data on u(x,t) are needed to estimate the background flow characteristics, direct measurements were made. The velocity components were measured using a standard three-component Acoustic Doppler Velocimeter (ADV). This instrument had a relatively low noise level ($\approx$ 0.2 cms^{-1}) and a small cylindrical (diameter 0.6 cm, height 0.3 cm) measurement volume ($\approx$ 0.1 cm^3) with a data collection frequency up to 25 Hz (for detail see Snyder & Castro, 1998). The wave elevations were measured using standard wave gauges. The ADV probe is attached to a long supporting rod, which is fixed to a carriage. The carriage is mounted on rails on top of the tank and has two degrees of freedom, traversing in the horizontal and vertical directions. In order to measure the Lagrangian displacement field in the water, small neutrally buoyant particles were introduced into the flow. To obtain representative data, the velocity and wave elevation records were phase averaged over 50-60 periods of oscillations. An example of such velocity measurements is shown in Fig. 11.

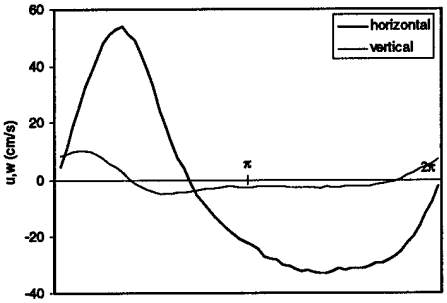

Figure 11. *Typical horizontal, u, and vertical, w, components of the water velocity under a periodic nonlinear wave along the slope. Section #25, depth is 10 cm above the bottom. The data are averaged over 50 wave periods and the wave period is 2.5 s.*

Horizontal velocity component u in the along flow direction x and the vertical component w in the vertical direction z are shown in Fig. 11. There is practically no water motion in the across flow direction y and this velocity component is not shown. As can be seen, although the paddle motion is purely sinusoidal, the water particle velocity components u and w become strongly asymmetric as the wave propagates along the slope. The measurements, similar to those shown in Fig. 11 were made in different sections of the tank and typical results for the horizontal along-slope water velocities u in sections 19-27 are shown in Fig. 12. As can be seen, the amplitude of the horizontal water velocity changes along the slope. The maximum velocity

increases, while the time interval in which the velocity is positive during each period decreases. This is the result of the wave steepening and related nonlinear effects.

As can be seen from the results of measurements presented above, the water motion in the tank is strongly asymmetric (in the onshore and offshore directions) and varies with the distance along the slope. These are the most important differences between the present case of nonlinear progressive shallow water waves propagating along a slope and much more simple cases of swash flow generated by a dam break method and of spatially independent oscillatory flow generated by large standing waves.

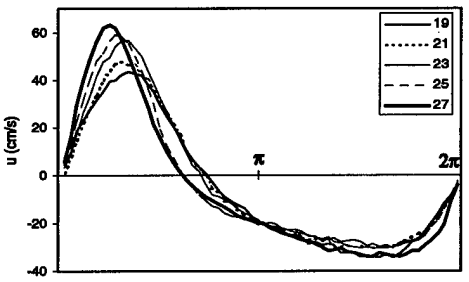

Figure 12. *Typical horizontal water particle velocities, u, as function of position in the wave tank. The data were taken in different sections at depth 10 cm from the bottom. Standard phase averaging was applied. The waves break in section #30. Section numbers are shown in the legend.*

The data, similar to those shown in Figs. 11, 12, were digitized and used as inputs for the model calculations, which are discussed below.

3. Cobbles/mines on impermeable bed

The results of experiments on the motion of cobbles/mines along horizontal and slopping solid beds for different background flows are now discussed. The general problem here may be formulated as follows. Let a cobble/mine rests on a solid bed and be subject to the action of (in general arbitrary) background flow. When the flow velocity exceeds some critical value the object starts moving. What are the critical conditions of the initiation of motion and how the object will move? The partial answers to these questions are given below.

Based on the results of numerous experiments conducted under simplified background flow conditions (swash flow and symmetric oscillatory flow) theoretical models were developed to describe the motion of heavy disks, spheres, spherical shells filled with liquid (to change the moment of inertia) in these basic time-dependent flows (Luccio et al., 1998; Voropayev et al., 1998). Using the proper theoretical parameterizations for the velocity in such flows, analytical solutions were derived in closed form and verified experimentally.

The models developed for these configurations are rather general and permit one to consider more complicated cases for which the background flow depends not only on time but on the spatial (along-slope) coordinate as well; i.e., the situation in a real surf zone or that modeled in the large wave tank (Figs.9, 10). In cases for which the background flow is primarily a function of time only, it was possible to derive analytical solutions describing the cobble/mine displacement. For the general case in which the background flow is a function of both time and the spatial coordinate (Figs. 11,12), analytical solutions were untenable and the resulting nonlinear, integro-differential equations for the cobble/mine motion were solved numerically.

Consider briefly a general case in which the background flow is a function of both time and the spatial coordinate (for details see Voropayev et al., 2001). A schematic of the system under consideration is shown in Fig. 13. Here u(x,t) is the background water velocity in the stream-wise or x-direction, U(t) cobble velocity, F_d drag force, F_L lift force, F_f dynamic bottom friction, F_p accelerating pressure term, $G = (M_C\text{-}M)g$ reduced gravity force, g gravitational acceleration, M_C mass of cobble, M water mass displaced by cobble, α slope angle, $F_G = G \sin\alpha$ and $F_N = G \cos\alpha$.

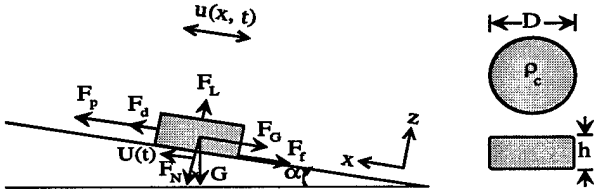

Figure 13. *Definition sketch with coordinate system and periodic forces that act on a cobble/mine placed on a sloping beach in a surf zone.*

Consider a disk-shaped cobble (Fig. 13) of diameter D, thickness h and density ρ_C initially ($t < 0$) at rest at $x_C = 0$, on a plane sloping at an angle α to the horizontal. At $t = 0$, the surrounding fluid of density ρ ($< \rho_C$) begins to move with an arbitrary velocity u(x,t) parallel to the floor. If the net force that acts on the cobble is not equal to zero, the cobble begins to move with a velocity $U = dx_C/dt$ in the direction of the x-axis.

The balance of momentum for a cobble in the stream-wise or x-direction gives

$$(M_c + K_m M)\frac{dU}{dt} = (1 + K_m)\,M\frac{du}{dt} + F_d - G\sin\alpha + F_f\,, \qquad (1)$$

(K_m is the virtual mass coefficient, $du/dt = \partial u/\partial t + u\partial u/\partial x$). Using standard parameterizations

$$F_d = \frac{1}{2}\rho S_1 C_d |u-U|(u-U),\quad F_f = -KE(G\cos\alpha - F_L)\frac{U}{|U|},\quad E = \begin{cases} 1, & G\cos\alpha > F_L, \\ 0, & G\cos\alpha \le F_L, \end{cases}$$

$$F_L = \frac{1}{2}\rho S_2 C_L (u-U)^2 \qquad M_c = \rho_c \frac{\pi D^2 h}{4},\ M = \rho\frac{\pi D^2 h}{4},$$

($S_1 = Dh$, $S_2 = \pi D^2/4$, C_d and C_L are the drag and lift coefficient, K is the kinetic friction coefficient) and denoting $\rho^* = \rho_C/\rho$, $\Delta = u - U$, which is the velocity of the cobble relative to the water velocity, and using the identity $d\Delta/dt = \partial\Delta/\partial t + U\partial\Delta/\partial x$, (1) takes the form

$$\begin{aligned}(\rho^* + K_m)\left(\frac{d\Delta}{dt} + \Delta\frac{\partial u}{\partial x}\right) + \frac{2C_d}{\pi D}\Delta|\Delta| &= (\rho^* - 1)\frac{du}{dt} + (\rho^* - 1)g\sin\alpha \\ + KE\frac{U}{|U|}\left\{(\rho^* - 1)g\cos\alpha - \frac{C_L}{2h}\Delta^2\right\}&\end{aligned} \qquad (2)$$

For the configuration considered, $C_L \approx C_d \approx C_0 \approx 0.6$ and $K_M = 1.2$ can be used (Yalin, 1977; Sarpkaya, 1986; Voropayev et al., 1998, 2001).

In non-dimensional variables

$$\begin{aligned} u^* &= \frac{u}{\varepsilon\omega}, \quad U^* = \frac{U}{\varepsilon\omega}, \quad \Delta^* = \frac{\Delta}{\varepsilon\omega}, \quad t^* = \omega t, \\ D^* &= \frac{D}{\varepsilon}, \quad h^* = \frac{h}{\varepsilon}, \quad \rho^* = \frac{\rho_C}{\rho}, \quad g^* = \frac{g}{\varepsilon\omega^2}, \end{aligned} \qquad (3)$$

(the amplitude ε and period $1/\omega$ of the paddle oscillations are used as the length and time scales) one obtains

$$\begin{aligned}(\rho^* + K_m)\left(\frac{d\Delta^*}{dt^*} + \Delta^*\frac{\partial u^*}{\partial x^*}\right) &= (\rho^* - 1)\frac{du^*}{dt^*} - \frac{2C_o}{\pi D^*}\Delta^*|\Delta^*| + (\rho^* - 1)g^*\sin\alpha \\ + KER\left\{(\rho^* - 1)g^*\cos\alpha - \frac{C_o}{2h^*}(\Delta^*)^2\right\}&\end{aligned}, \qquad (4)$$

where

$$E = \begin{cases} 1, & (\rho^* - 1)g^*\cos\alpha > \dfrac{C_0}{2h^*}\Delta^{*2} \\ 0, & (\rho^* - 1)g^*\cos\alpha \le \dfrac{C_0}{2h^*}\Delta^{*2} \end{cases}, \qquad R = \frac{U^*}{|U^*|} = \frac{u^* - \Delta^*}{|u^* - \Delta^*|}. \qquad (5)$$

When u does not depend on the spatial coordinate ($\partial u/\partial x = 0$), the solution for Δ^* may be found analytically and the non-dimensional cobble displacement $x_c^* = x_c/\varepsilon$ is given by

$$x_c^* = \int_0^{t^*} U^* dt^* = \int_0^{t^*} u^* dt^* - \int_0^{t^*} \Delta^* dt^*. \qquad (6)$$

Some examples of practical interest are given in Luccio et al. (1998) and Voropayev et al. (1998).

If the form of background velocity u(x,t) is known, for example, from direct measurements as in our case, then the system of equations may be closed. Choosing the initial conditions, for example, as

$$\Delta^* = \Delta^*(0) \quad \text{and} \quad x^* = x^*_C = x^*_C(0) \qquad \text{at } t^* = 0,$$

the governing equation (4) can be solved using a fourth order standard Runge-Kutta method and cobble positions may be calculated. For this purpose digitized experimental data, similar to those shown in Figs. 11, 12, were used as inputs for u(x,t) in the model calculations.

In the experiments cobbles/mines of different sizes were placed along the floor in a wave tank (Fig. 8) with model surf flow and their evolution with time was studied and compared with the model predictions. Onshore and offshore mean motions of cobbles as well as steady oscillations with zero mean displacement were observed for different conditions and two typical examples are shown in Figs. 14, 15.

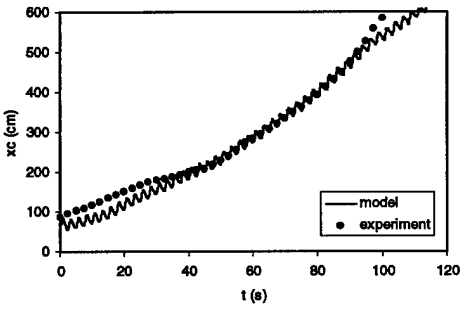

Figure 14. *Averaged over one wave period cobble position x_C as a function of time t for a medium-size cobble (cobble B in Table 1).*

Figure 15. Mine position x_C as a function of time t for a large model mine (mine 2 in Table 1) provided by NRL. Experimental data were taken using high-resolution digital imaging.

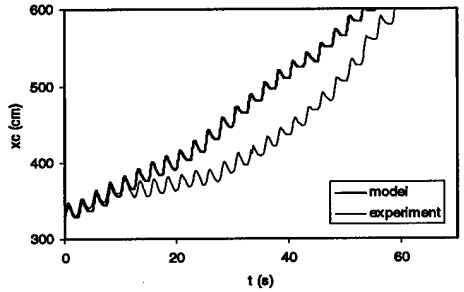

For the range of parameters used in the experiments, satisfactory agreement between the measured and calculated values of the cobble/mine displacements as a function of time was obtained in other experiments including case when one of the cobbles was lifted (at least partly from the bottom as it moves forward in section #29.

Figure 16. A photograph showing the separation of cobble 2 (replica of anti-tank mine) from bed during onshore (from right to left) stage of motion.

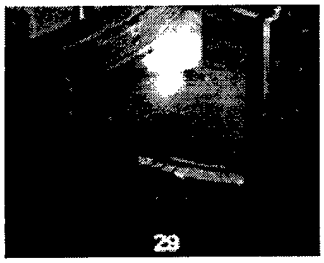

Overall, the behavior of cobbles on a slope depends on the cobble size, density and initial cobble position. For the wave parameters used in the experiments, the cobble/mine does not move at all when its density is relatively large ($\rho_C > 1.5$ gcm^{-3}). In this case the (static) friction force exceeds the net driving force from the surrounding fluid at any position of cobble on the slope. We could not increase significantly the driving force from the surrounding fluid (wave amplitudes) without the corresponding loses of wave stability and for this reason cobbles with smaller densities (see Table 1) were used in these experiments. These lighter cobbles can move along the slope, mostly onshore, but in general their direction of motion may depend on the initial cobble position and cobble parameters (see details in Voropayev et al., 2001).

4. Sandy bed morphodynamics

In these studies a layer of sand (thickness 20-25 cm) was placed on the bed. Two kinds of quartz sand (density ρ_s =2.6 gcm^{-3}, mean grain size d = 0.04 cm and 0.1 cm) were used in the

experiments. The sand surface was leveled and the background flow was initiated. Particular attention was paid to the instability of the sand-water interface, formation of sand ripples and bar and temporal evolution of the bottom morphology at different background flow conditions. Two series of experiments were done. The first series was conducted in symmetric oscillatory flow using standing wave tank (Fig. 7) with horizontal bottom. Second series of experiments was done in a model surf flow reproduced in a large wave tank with a slope (Fig. 8).

The general problem here may be formulated as follows. Let initially flat layer of sand (on a horizontal or sloping bottom) is subjected to the action of a periodic background flow. It is well known that at some critical conditions large vortex ripples and bars are formed at the sand surface. How fast these ripples and bars are formed, what are their quasi-steady characteristics, their migration velocity in different flow conditions? Partial answers on these questions are given below/

Qualitative observations of the experiments can be summarized as follows. After the waves are generated, an oscillatory shear stress is developed near initially flat bottom (Fig. 17a) and rolling grain sediment transport was observed when the velocity amplitude exceeds a critical value. Owing to the instability at the water-sand interface, small (typical height 0.5 cm) three-dimensional ripples (typical horizontal spacing of 4-5 cm) are generated at the bed. With time, the height of the initial 3D ripples increases; the ripples then merge, forming the well-known 2D vortex ripples oriented across the flow (Fig. 17b).

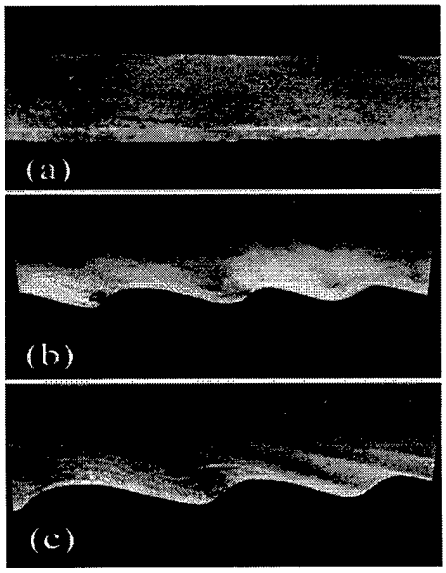

Figure 17. *Side view photographs showing (a) - initially flat sandy bottom; (b) - growing and (c)- quasi-steady sand ripples formed on a slope under progressive waves with relatively large intensity.. The horizontal size of frames, 61 cm, gives a length scale.*

These 2D ripples initially have a relatively small height h(t) and spacing L(t), but with time their size increases and, after an adjustment time interval (see below), they reach a quasi-steady equilibrium state (Fig. 17c) with a characteristic height h_0 and spacing L_0. With increasing ripple size and height to length ratio, h/L, the flow around the ripples becomes turbulent and intense, and vortices are periodically generated near the ripple crests. Ripples in this stage are called the "vortex ripples." When the waves are symmetric (relative to the vertical plane), as in the case of large symmetric standing waves, vortices are formed periodically and symmetrically at both sides of the ripples which also tend to be symmetric (Fig. 2). Similar (but slightly asymmetric) ripples are also observed for progressive waves on a slope far offshore from the break point where the wave asymmetry is relatively small. When the wave asymmetry increases, the vortices are formed mostly at the onshore side of the ripple while they do not occur at the offshore side; the resulting ripples are strongly asymmetric (Fig. 17c).

Note that for symmetric flow ripple generation occurs uniformly along the horizontal bed. For progressive waves on a slope, at early times 3D ripples are generated rapidly just offshore of the breaking point were the velocity amplitude has its maximum. The ripple-formation zone then propagates as a front in the offshore (down-slope) direction; after some time the entire slope is covered with ripples (Fig. 18).

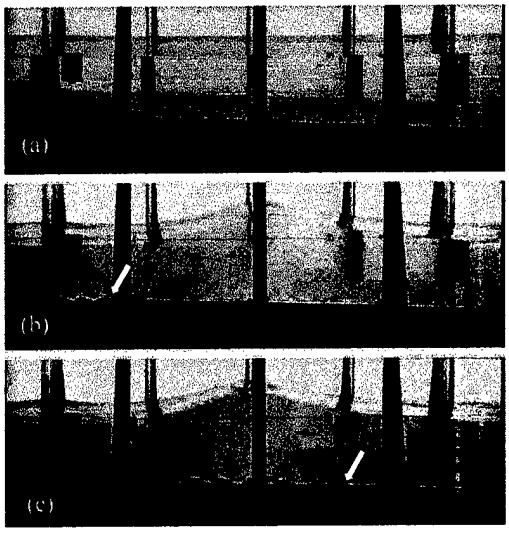

Figure 18. *Ripple front (shown by arrow) propagating (b, c) along initially flat slope (a) in the offshore (from left to right) direction under progressive waves on a slop.*

The front propagation velocity strongly depends on the wave characteristics and water depth and decreases with the distance X from the break point. If the waves are not very

energetic, than after some typical time, t_0, the ripple front stops propagating along the slope at a distance S_0 from the point of ripple formation near the break point. As a result, part of the slope is covered with ripples while the rest remains flat for a long time (4-5 hours). For very energetic waves, X_0 is rather large and ripple front propagates along the entire slope. Experimental data on the front propagation were collected and explained using a model developed by the present investigators. The underlying concept of the model is that the ripple height h increases with time in accordance with (7) (see below) while characteristic time τ vary along the slope in accordance with the background flow variation (h_0 increases and τ decreases in the offshore direction). As a result, the non-dimensional front distance increases with time as

$$X/X_0 = 1 - \exp(-t/\tau),$$

where τ is a characteristic time that depends on the wave frequency and mobility parameter (see details in Voropayev et al., 2003).

Analyses of experimental data (see Fig. 19) show that in both cases (horizontal bed and sloping bed) the non-dimensional length L/L_0 and height h/h_0 of the generated ripples increase with the non-dimensional time t/τ as

$$L/L_0 = 1-\exp(-t/\tau), \qquad h/h_0 = 1-\exp(-t/\tau), \qquad (7)$$

where L and h are the ripple current length and height, and L_0 and h_0 are their equilibrium quasi-steady values, which may be calculated using well known empirical formulas (see, e.g., Sleath, 1984, O'Donoghue & Clubb, 2001) and

$$\tau = C/\omega\psi^{1/2}$$

is a characteristic time scale for ripple formation introduced in Voropayev et al. (1999, 2003). Here ω is the wave frequency, C = 2500 is an empirical constant and ψ is the mobility parameter, defined as

$$\psi = U^2/g(s-1)d \qquad (8)$$

($s = \rho_s/\rho$, d is the mean sediment diameter, g is the gravitational acceleration, U is the amplitude of fluid velocity).

The main difference between two cases is that for a horizontal bed (Fig 19a) ψ doesn't depend on the position x along the bed, while for a slope (Fig. 19b) ψ increases along the slope in the onshore direction (because the maximum along flow velocity U increases).

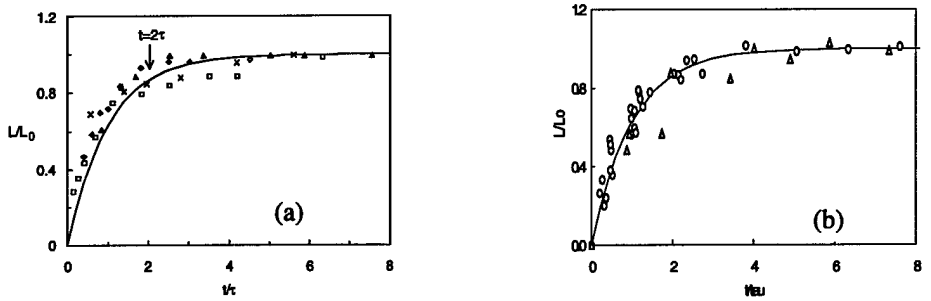

Figure 19. *The non-dimensional ripple lengths L/L_0 as functions of the non-dimensional time t/τ for different experiments (symbols) conducted with (a) oscillatory flow on horizontal bed, (b)with progressive waves along the slope. The solid line shows the approximation function (7). In (b) the data were taken at different incoming wave characteristics and in different sections along the slope and changes in the values of ψ tv (8) were taken into account.*

Using the conservation of the flux of wave energy in the direction of waves propagation and some other general arguments, the changes in U along the slope may be estimated theoretically (see example in Fig. 20 and details in Voropayev et al., 2003) and local values of Ψ in (8) and L in (7) can be accurately calculated (Fig. 19b). It is also shown in the mentioned paper that when the wave intensity increases, τ strongly decreases, implying that for more energetic ripples are formed faster and reach a quasi-steady state earlier. This explains why in experiments with sandy slopes the ripple formation zone forms a front that separates ripples from the smooth sandy bottom near the break point.

Figure 20. *A typical distribution of the maximum water velocity, U, along the slope. Symbols - measured values, solid line - theoretical estimates. Experimental parameters: ω= 0.4 Hz, ε_0 =5 cm. Waves break in section #31.*

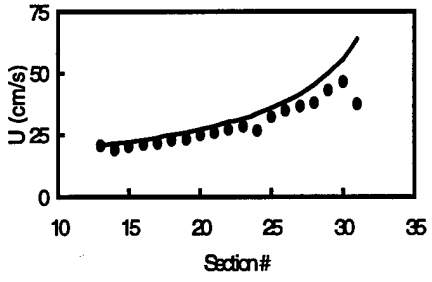

At large times $t >> \tau$ the morphology of the ripple bed continues to change, although the mean ripple characteristics L_0 and h_0 (at a fixed position along the slope) do not change appreciably after the formation period 2τ; i.e. the bottom topography never reaches an exact

steady state. While the frequency and amplitude of paddle oscillations remain constant, the ripples generated on the bed demonstrate large time instabilities.

The first type of instability is related to the periodic merger and split of ripples (Fig. 21). This effect was observed and explained for the case of a horizontal sandy bed under spatially homogeneous oscillatory flow in Voropayev et al. (1999).

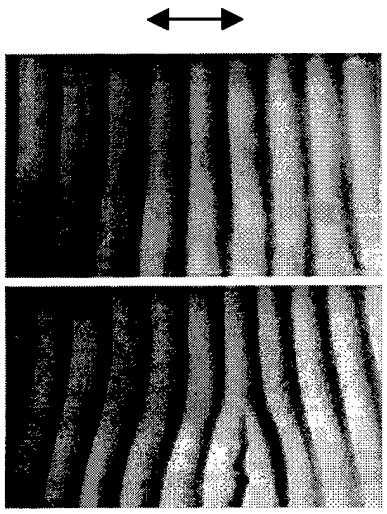

Figure 21. *Plan view photographs showing a regular system of ripples in quasi-steady state (a) and the large-time instability of the bottom topography and formation of a new ripple (b). With time the newly formed ripple spreads along the bed across the flow and initiates small mean drift of the surrounding ripples. Arrows show the flow directions.*

This process (Fig. 21) resembles the appearance of periodic dislocations in an initially regular ripple pattern. The dislocation induces migration of ripples in the proximity, and with time the new or merged ripples spread across the flow. Because the typical spacing between ripples decreases/increases during ripple merging/splitting, the whole system of ripples migrates with some typical "stochastic" drift velocity U^*_d. With time, a new quasi-steady state with approximately the same typical spacing, L_0, between ripples and height, h_0, is established. In spatially homogeneous oscillatory flow, the migration velocity has no preferred direction and the mean drift velocity as averaged over large times tends to be zero. The typical *absolute* value of this velocity for ripples over a horizontal bottom may be estimated as (Voropayev et al., 1999)

$$U_d^* = U\Psi^{1/2}(2.2 - 0.35\Psi^{1/3})/8C. \qquad (9)$$

The observations collected in the model surf zone show that, in addition to the above-mentioned instability, another type of instability is possible under progressive waves on sloping beaches. This instability causes a steady onshore ripple drift with unidirectional drift velocity, U_d, along the slope. Using the model proposed by Kennedy (1963) and Engelung (1970) (see

also Nielsen, 1992, p. 133) for sediment transport resulting from unidirectional drift of sinusoidal bedform with constant shape, the value of U_d was estimated as (Voropayev et al., 2003)

$$U_d = \omega d^2(\Psi/10)^{3/2}/nh_0 \qquad (10)$$

(n is the volume of solid fraction in a unit volume of the bed, for sand, $n \approx 0.7$). The data on U_d were collected for different along slope positions (section #), and typical results for one experiment are shown in Fig. 22. The estimates based on (10) (where *local* values of ε and U were used to calculate *local* Ψ) are shown by solid lines.

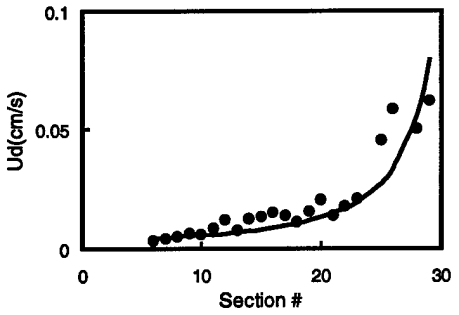

Figure 22. *Unidirectional ripple drift velocity, U_d, as a function of the along slope position. Symbols show measured values for an experiment with $\omega = 0.4$ Hz, $\varepsilon_0 = 10$ cm, solid line shows the estimation based on (10).*

To gain a better understanding of sediment transport and ripple drift, the flow around ripples was investigated. Recently, Ridler & Sleath (2000) reported observations on the Eulerian time-mean drift induced by waves over solid artificial ripples placed at the bottom of a water layer of constant depth. In their work, velocity measurements were taken at different distances from a crest and a trough and then phase averaged. A mean negative (offshore) water drift was observed near the bed over ripple troughs. Just above the ripple crests in the boundary layer, however, a positive (onshore) mean water drift was documented. No similar data exists for naturally formed (moving) sand ripples. Owing to the drift and spatial variability of sand ripples, however these measurements are more intricate and some results are described below.

The ADV probe was placed in the middle of the tank in section #27 (Fig. 23). In addition to the velocity, the ADV probe can measure the distance to the bottom with an accuracy better than 0.1 cm. Using this latter capability, measurements of the ripple profile were taken every 10 s while ripples are drifting onshore under the stationary probe (Fig. 23).

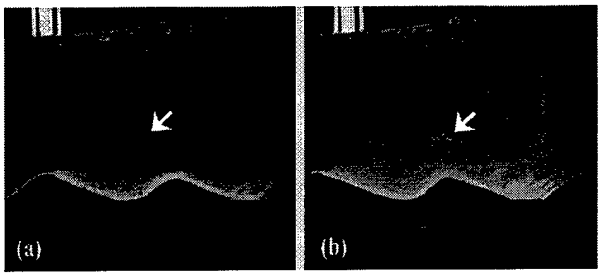

Figure 23. *Side view photograph (digitized image from video) showing the ADV probe above the drifting (from right to left) sand ripples. Experimental parameters: ω = 0.4 Hz, ε_0 = 10 cm, section #27. Frame (b) was taken 2.5 min after the frame (a). The ADV probe is barely visible and is shown by an arrow.*

Using these data and measuring the ripple length, the averaged ripple drift velocity over the measurement period was calculated as $U_d = 0.048$ cms^{-1}. After collecting data on the ripple profile and drift, the ADV probe was rapidly traversed horizontally so that its measuring volume is at a location just above the ripple crest. Then the velocity measurements were taken while ripples drifted onshore. Figure 24 gives typical horizontal velocity traces. The data shown in Fig. 24a were taken approximately 5 cm above the ripple trough at the level of the ripple crest and the data shown in Fig. 24b were taken in the boundary layer approximately just above the ripple crest. The velocity magnitude at 5 cm above the trough is approximately two times larger than in the boundary layer above the crest. The averaged velocity over a wave period above the trough (Fig. 24a) is negative (offshore) while it is strongly positive just above the ripple crest (onshore) (Fig. 24b), pointing to the possibility of significant onshore sediment transport and hence a corresponding ripple drift.

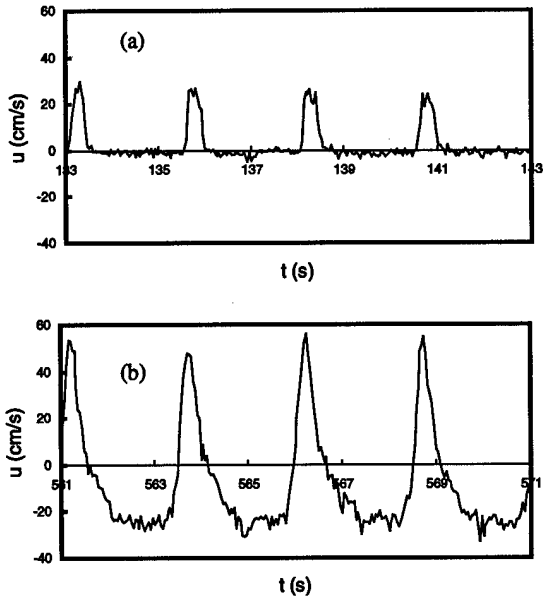

Figure 24. *Typical examples of horizontal along-slope velocity traces as obtained in the boundary layer above the ripple crest (a) and approximately 5 cm above the ripple trough at the level of ripple crest (b). The velocity magnitude above the trough (b) is approximately twice larger than in the boundary layer above the crest (a). As can be seen, averaged (over the wave period) velocity above the trough (b) is negative, while it is strongly positive just above the ripple crest (a). Time is given in accordance with Fig. 25 below. Experimental conditions are the same as in Fig. 23.*

The data in Fig. 24 present short pieces of a rather long time record collected while the ripple drifted approximately a distance L_0 under the ADV probe. These data were time-averaged over five wave periods and the results are shown in Fig. 25. Note the positive mean water drift just above the ripple crest. This result is consistent with the measurements over solid ripples by Ridler & Sleath (2000) and justifies the use of (10) for estimating ripple drift velocity.

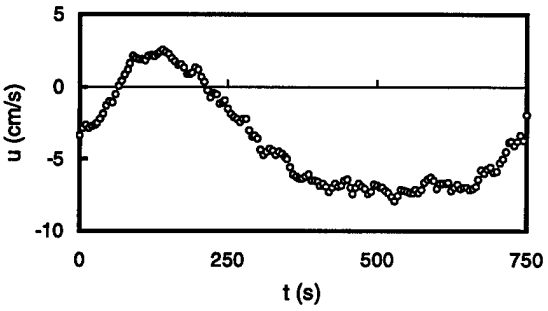

Figure 25. *Time record of the along-slope velocity component, u, averaged over five wave periods and taken at a level just above the ripple crest when the ripple slowly drifted one ripple length L_0 under the ADV probe. Experimental parameters are same as in Fig. 23*

In order to better understand cobble-sandbar interactions (which are discussed in the next section), experiments were conducted on the formation and evolution of sandbars on an initially flat sandy slope. In the range of parameters used in experiments at least two different types of sandbars were observed, namely onshore moving sandbars and offshore moving sandbars. The type of breaker on a sloping beach depends on the beach slope and wave parameters. Battjes (1974) characterizes the waves by the surf similarity parameter

$$\xi = \tan\alpha / \sqrt{\eta^*/\lambda},$$

where α is the slope angle, η^* wave amplitude near the break and λ wavelength in deep water. Accordingly, a spilling breaker occurs when $\xi < 0.4$, a plunging breaker occurs when $0.4 < \xi < 2.0$ and a surging breaker occurs at larger ξ. Depending on the range of parameters used in the experiments, spilling or plunging breakers can be generated, leading to different sandbar types; an example of a sandbar under a spilling breaker is shown in Fig. 26a, which has a bump-like shape. In this case, even after breaking, waves are still energetic enough to form a large vortex onshore of the accumulated sand, causing offshore sediment motion and slow offshore drift of the bar. Note that this opposes the sediment transported by the onshore migrating ripples offshore of the bar. In the case of a plunging breaker (Fig. 26b), sandbars of trapezoidal shape are formed. They have flat tops, small height and larger widths. Plunging breakers form closer to the shoreline and significant amount of energy is dissipated by a large vortex. The flow is not

energetic enough to form another large vortex onshore side of the accumulated sand. Therefore, onshore mean sediment transport is observed and, as result, bar slowly expands in the onshore direction.

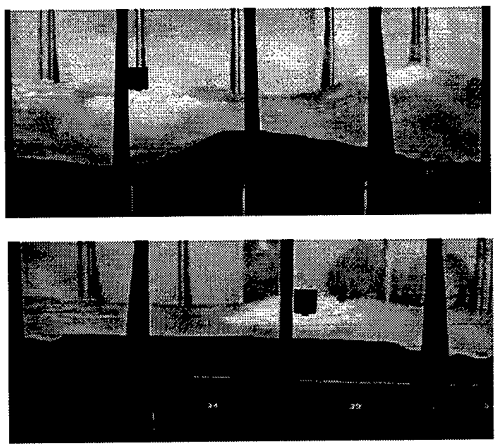

Figure 26. *Two typical examples of sandbars formed under spilling (a) or plunging (b) breakers. Experimental parameters: ω = 0.75 Hz, ε_0 = 7.5 cm (a), 0.6, 5 (b). Time is approximately t = 140 min (a), 75 (b) from the beginning of the experiment.*

5. Cobbles on sandy bed

Upon completion of detailed studies on the sand bottom morphodynamics, model cobbles/mines were placed at the slope and their behavior, including scouring and burial, was investigated. The experiments were initiated with a smooth sandy bottom. When the system reached its quasi-steady state, with established ripples, cobbles were dropped on the bed and their behavior was monitored. Since the flow velocity around the cobble increases relative to the background flow, scouring of the bed can be initiated. The results of experiments show (Fig. 27) that the maximum subsidence, S, of the cobble is not very significant and doesn't depend on the cobble density and height, but depends mostly on the cobble diameter, D, and may be estimated as S = 0.15D (Voropayev et al., 1999). At the same time, sediment from the nearest ripples is transported towards the cobble, thus significantly changing the bottom topography close to the cobble and burying the cobble under migrating ripples (Fig. 28). Thus, the scouring appeared to be of lesser importance as compared to the migration of ripples.

This phenomenon (ripple migration) leads to periodic burial of cobbles by migrating ripples. Typical period of such burial can be estimated as $T_b = L_0/U_d$, which is the time for a system of ripples to drift with a velocity U_d a distance equal to one ripple length L_0 (see schematic in Fig. 29). Estimates show that, for example, for conditions used in the experiment in Fig, 27, T_b = 6.5 min, which is in agreement with the observations. For the typical oceanic

conditions (wave amplitude 1 m, period 10 s, depth 10 m, sand size 0.1 cm) estimates also show (Voropayev et al., 1999) that a mine of diameter 20 cm and height 10 cm may be completely buried after a typical time on the order of 4 hours, which is in agreement with the reported field data on ripple migration (Traycovski et al., 1999).

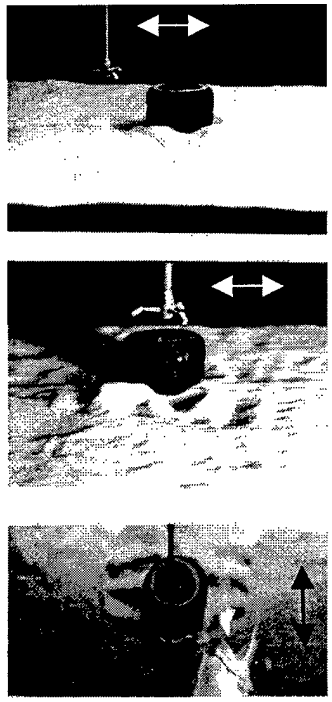

Figure 27. *Front view (a, b) and plan view (c) showing the scour pattern evolution near the cobble in steady oscillatory flow. Three-dimensional small-scale rolling grain ripples are also visible away from the cobble in (b). Arrows show the directions of the flow. Experimental parameters:* U_0 = 15 cms^{-1}, d = 0.04 cm, D = 10 cm, H = 6 cm. ρ_c = 2.0 $gmcm^{-3}$, *time* t = 5 min (a), 55 min (b,c) *after the beginning of the experiment. The ADV probe is also shown on these photographs.*

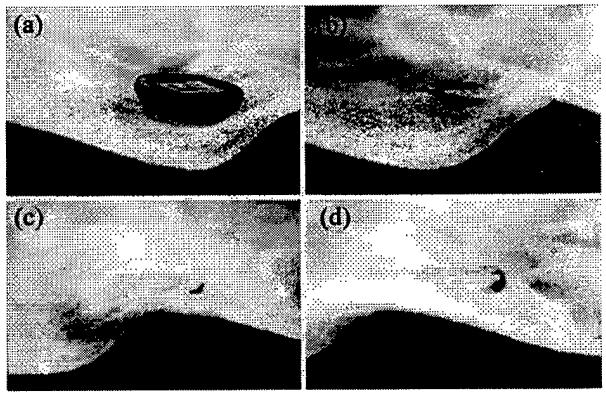

Figure. 28. *Periodic burial of relatively small, D = 8 cm, cobble that was trapped between two adjacent migrating ripples. Time interval between frames (a) and (d) is 6 min.*

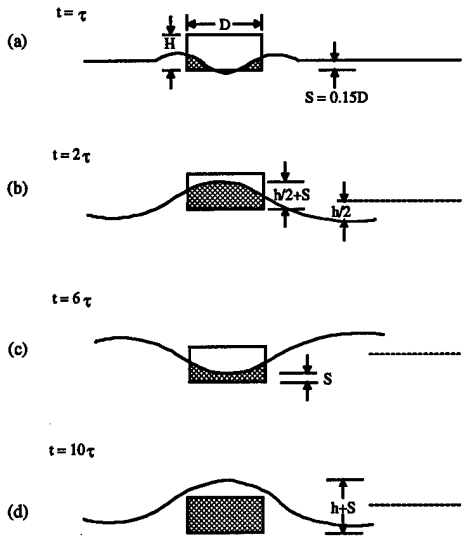

Figure 29. *Schematic showing the time behavior of a cobble/mine, which was placed on a sandy bed in oscillatory flow: (a) local scour and subsidence of cobble; (b-d) periodical burial of cobble under migrating sand ripples.*

Another topic that continues to being addressed in our research is sand bar interaction with large solid objects. As mentioned, at large times a sand bar of size much larger than the cobble is established under the breaking waves (see Fig. 26). The water depth decreases rapidly along the slope of the bar, and hence the flow becomes more energetic and provides enough momentum for the cobbles to climb along the sloping bar and reach its top.

If the incoming wave characteristics remain fixed, a quasi-equilibrium state can be established during which the cobbles stay near the top of the bar for a period of time (in experiments 0.5 hour or more); they, however, oscillate back and forth under the wave action (Fig. 30a). This observation can be explained as follows. The onshore water motion above the bar is very energetic and forces the cobble onshore. In addition, the incoming waves break here and a large vortex is formed under the wave crest, resulting in an intense turbulent bore that propagates onshore (swash flow). Return flow in the swash is less energetic, yet sufficiently strong and propagates near the bottom under the bore. The returning swash flow and the offshore motion (generated under the wave trough) cause the cobble to move offshore, following its onshore motion.

The oscillations of the cobbles at the top of the bar occur by these two competing mechanisms. This position, however, is unstable. Due to intense turbulent motion, the cobble may tip and slide down along the bar. When the cobble slides to the offshore side of the bar, it is

usually pushed back to the top of the bar and start oscillating again. If it slides along the onshore side of the bar, the cobble can either be pushed back to the top of the bar or get entrapped there.

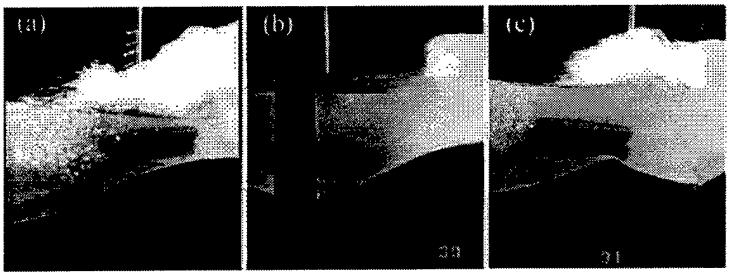

Figure 30. *Large and relatively light cobble, which was initially above the sand bar when the incoming wave characteristics were changed. The cobble oscillates steadily above the bar (a), then it slides to the trough at the onshore side of the bar (b) and finally moves steadily onshore (c), reaching with time the shoreline (not shown). Cobble 2 was used in this run (see Table 1).*

Changing of incoming wave characteristics alters the position of the break point and hence the behavior of cobbles. The associated processes are intricate, and here we present an example to illustrate this complexity.

Figure 31. *The burial of a large and relatively heavy cobble, which initially was above the sand bar when the incoming wave characteristics were changed. The cobble (a) slides to the trough at the onshore side of the bar and is slowly buried (b) under the drifting bar. Cobble 3 was used in this run.*

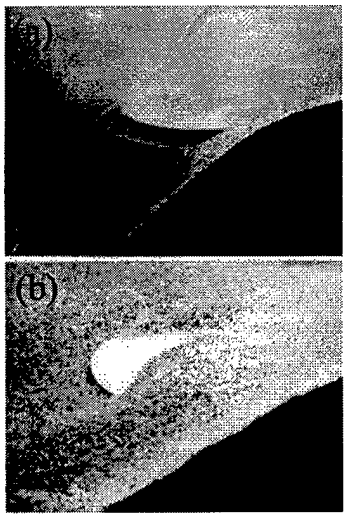

When the wave characteristics are changed to a lower frequency or smaller amplitude, the waves break closer to the coastline and the bar drifts onshore. Thence, the back flow above the bar is significantly reduced and the cobble slides down from the bar crest along the onshore side

(Fig. 30b). The general behavior of cobble depends on the cobble density. If the cobble is relatively light, it moves slowly onshore, reaches the swash region and (usually) continues to move (Fig. 30c) under the turbulent bore until it arrives at the shoreline. If the cobble is relatively heavy, it tends to be trapped in the onshore face of the bar. Because of the slow onshore migration of the bar, the cobble can be completely buried under the bar, as shown in Fig. 31, for a long period of time. This burial process is rather slow and can take several hours in laboratory.

6. Conclusions

The main finding of this research may be summarized briefly as follows.

A. In the first phase of the research, the motion of cobbles/mines in a swash zone on an impermeable slope was modeled experimentally and analyzed theoretically. In oceanic situations, the beach is, of course, permeable. Owing to the fact that very little research has been done on this problem, it was decided to first investigate the more simplified case of an impermeable bottom. This allowed considering a physical system with a reduced number of external parameters, yet one which captured the main features of oceanic situations. Even with this simplified problem, at least ten external parameters ($H_0, D, h_c, \rho_c, \rho, \nu, g, \alpha, K$ and t) were shown to be important. In the experiments, a dam-break flow was used to simulate an impulsive swash. It is shown that, when the threshold for the initiation of motion is exceeded, the cobble starts to move with relatively large velocity in the on-shore direction. The cobble displacements were measured as a function of time and all other external parameters. Based on the results of experiments a physical understanding was obtained and a theoretical model was proposed to calculate cobble displacements. Satisfactory agreement between the laboratory observations and the model predictions was obtained.

B. The bottom motion of spherical and disk-shaped cobbles in a wave-induced oscillatory flow was studied experimentally and analyzed theoretically. In the experiments, large standing waves were used to model an oscillatory background flow that occurs near the surf zone. It is shown that the cobble motions in such a flow rapidly become periodic with reduced amplitude compared to the background flow; a phase shift between the cobble and background flow displacements is also evident. The cobble displacements, as a function of time and other (at least ten) external parameters, were measured. Based on the results of the experiments, a model was

developed and the cobble displacements were calculated and compared with measured values. The model also allowed calculating the rather complex behavior of the angular velocity of the spherical cobbles. The purpose was not only to make measurements relevant to the dynamics of cobble in oscillatory flow, but also to understand the basic physics and verify a theoretical model. To reduce the number of governing parameters, a simplified geometry with a solid bottom, was chosen and a model (which still includes at least ten parameters: D, ρ_c, h_c, K, g, $\rho, \nu, \omega, \varepsilon$, t) was developed.

C. The flow in the entire surf zone was modeled in a large wave tank and the motion of cobbles/mines along an impermeable slope was studied under time and spatial dependent flow conditions. Onshore and offshore motions of cobbles, as well as steady oscillations with zero mean displacement, were observed for different conditions. To explain the results of observations, the models developed in A and B were generalized for these more complicated conditions. Proper parameterizations were used for the pressure accelerating term, drag, lift and other nonlinear forces. Comparison of measured and calculated values for the cobble displacement shows that the model correctly predicts the cobble behavior in model surf. One of the key variables in the model, which is known with the least accuracy, is the virtual mass coefficient of a disc moving with variable velocity along a solid boundary. A fixed value for this coefficient, as well as for the drag and lift coefficients was used in the calculations. It is important that in calculations the spatial variation of the background velocity along the slope must be taken into account. Proper parameterization for this effect was proposed and used.

D. The behavior of cobbles/mines placed on a horizontal sandy bed in an oscillatory flow was studied experimentally. It is shown that when the background velocity is below its critical value, small-scale rolling-grain ripples develop on an initially flat bottom and noticeable scour around the cobble occurs. At large times the scour pattern reaches a quasi-steady state and the estimates for the resulting maximum subsidence of the cobble are derived. When the background velocity exceeds its critical value, vortex ripples start to form. The typical time of ripple formation depends on the wave frequency and the mobility parameter, and can be estimated using proposed parameterizations. At larger times the system of ripples is not stable and they migrate with some drift velocity. As a result a heavy cobble may be buried periodically. The data on the ripple drift velocity were collected and parameterized. Basing on this parameterization the estimates for the time of periodic cobble burial were derived.

E. The evolution of an initially flat sandy slope and the behavior of disk-shaped cobbles in model surf zone were studied experimentally. The experiments were conducted in a large wave tank with a sandy slope. Upon initiation of wave forcing, the initially flat topography changes and after a transitional time, the bedform reaches a quasi-steady state with a system of sand ripples and a large bar near the break. Although the incoming wave characteristics are fixed, the bottom topography never reaches a full steady state but evolves slowly (e.g. ripple drift and sandbar transformation at large times). The data on the ripple formation, growth, drift, and quasi-steady ripple characteristics were collected and compared with proposed theoretical predictions. When the incoming wave characteristics were changed, the bottom topography responded by establishing a new quasi-steady state after a certain adjustment time period. The above studies were extended to include cobbles/mines placed along the sandy slope. Four different scenarios were identified and explained: (i) steady oscillations of cobbles with zero mean displacement and small scour; (ii) mean onshore motion of relatively light cobbles, (iii) periodic burial of relatively heavy cobbles of which the dimensions are comparable to that of sand ripples, (iv) burial of relatively large cobbles under the bar when the break point was changed by changing incoming wave characteristics. Physical explanations were provided to explain the observations. Data on the flow characteristics in the vicinity of the movable bed were also obtained. The presence of a mean onshore flow in the boundary layer above the ripple crest was observed, corroborating recent observations of Ridler & Sleath (2000) carried out in the wave boundary layer above solid sinusoidal bedforms.

7. References

Arcilla, A.S., Stive, M.J.F. and Kraus, N.C. (Editors) 1994. *Coastal Dynamics '94*. Amer. Society of Civil Eng., New York.

Battjes, J.A. 1974. Surf similarity. *Proc. 14th Coastal Eng. Conf.,* Amer. Society of Civil Eng., New York, 466-480.

Battjes, J.A. 1988. Surf-zone dynamics. *Ann. Rev. Fluid Mech.*, **20**, 257-293.

Belorgey, M., Rajaana, R.D. and Sleath, J.F.A. (Editors) 1993. *Sediment Transport Mechanisms in Coastal Environments and Rivers*. World Scientific, Singapore.

Blondeaux, P. 1990. Sand ripples under sea waves. Part 1. Ripple formation. *J. Fluid Mech.*, **218**,1-17.

Blondeaux, P., Foti, E. and Vittori, G. 2000. Migrating sea ripples. *Europ. J. Mech. B-Fluids,* 19 (2), 285-301.

Craik, A.D. 1985. *Waves Interactions and Fluid Flow*. Cambridge University Press, Cambridge.

Dean, R.G. and Dalrymple, R.A. 1994. *Water Waves Mechanics for Engineers and Scientists*. World Scientific.

Engelung, F. 1970. Instability of erodible beds. *J. Fluid Mech.*, **42**, 225-244.

Engelund, F. and Fredsoe, J. 1982. Sediment ripples and dunes. *Ann. Rev. Fluid Mech.*, **14**, 13-37.

Flick, R.E. and Guza, R.T. 1980. Paddle generated waves in laboratory channels. *J. Waterway, Port,* **106**, 79-97.

Fontanet, P. 1961. Theorie de la génération de la houle cylindrique par un batteur plan. *La Houille Blanche*, **16**(1), 3-31.

Fredsoe, J. and Deigaard R. 1992. *Mechanics of Coastal Sediment Transport.* Advanced Series on Ocean Engineering, V. 3, World Scientific, Singapore.

Grilli, S.T., Voropayev, S.I., Testik, F.Y., Fernando, H.J.S., 2003. Numerical modeling and experiments of wave shoaling over semi-buried cylinders in sandy bottom. *Proc. 13th Intern. Offshore and Polar Engineering Conference*, Honolulu, accepted for publication.

Horikawa, K. and Wanatabe, A. 1967. A study of sand movement due to wave action. *Coastal Engng. Japan,* **10**, 39-57.

Kennedy, J.F. 1963. The mechanics of dunes and antidunes in erodible-bed chanals. *J. Fluid Mech.*, **16**, 521-544.

Longuet-Higgins, M.S. and Stewart, R.W. 1964. Radiation stress in water waves; a physical discussion with applications. *Deep-Sea Res.*, **11**, 529-562.

Lott, D.F. and Poeckert, R.M. 1996. Extending cooperative research. Canada, New Zealand, United States in joint effort in British Columbia to evaluate penetrometers for ground-truthing acoustic classifiers for mine countermeasures. *Sea Technology*, **9**, 56-61.

Luccio, P.A., Voropayev, S.I., Fernando, H.J.S. Boyer, D.L. and Houston, W.N. 1998. Motion of cobbles in the swash zone on an impermeable slope. *Coastal Eng.,* 33, 41-60.

Madsen, O.S. 1971. On the generation of long waves. *J. Geophys. Res.*, **76**, 36, 8672-8683.

Mei, C.C. 1982. *The Applied Dynamics of Ocean Surface Waves*. John Wiley & Sons, New York.

Mei, C. C. 1985. Resonance reflection of surface water waves by periodic sand bars. *J Fluid Mech.*, **152**, 315-337.

Mei, C.C. and Liu, P.L. 1993. Surface waves and coastal dynamics. *Ann. Rev. Fluid Mech.*, **25**, 2-5-240.

Mei, C. C. and Yu, J. 1997. Note on the instability of sand ripples under partially standing surface waves. *Phys. Fluids,* **9**, 1606-1620.

Nielsen, P. 1992. *Coastal Bottom Boundary Layer and Sediment Transport.* World Scientific, London.

O'Donoghue, T., Clubb, G.S. 2001. Sand ripples generated by oscillating flow. *Coastal Engineering*, submitted.

Peregrina, D.H. 1983. Breaking waves on beaches. *Ann. Rev. Fluid Mech.*, **15**, 149-173.

Ridler, E.L., Sleath, J.F.A. 2000. Effect of bed roughness on time-mean drift induced by waves. *J. Waterway, Port, Coastal and Ocean Eng.*, **126**(1), 23-29.

Sarpkaya, T. 1986. Force on a circular cylinder in a viscous oscillatory flow at low Keulegan-Carpenter numbers. *J. Fluid Mech.*, **165**, 61-71.

Sleath, J.F.A. 1976. On rolling grain ripples. *J. Hydraul. Res.*, **14**, 69-81.

Sleath, J.F.A. 1984. *Sea Bed Mechanics.* Wiley Interscience, New York.

Sleath, J.F.A. 1995. Sediment transport by waves and currents. *J. Geophys. Res.,* **100**(C6), 10977-1098.

Snyder, W.H. and Castro, P.I. 1999. Acoustic-Doppler-velocimeter evaluation in a stratified tank. *J. Hydraulic Eng.*, ASCE, **125**(6), 595-603.

Svendsen, I. A. 1985. Physical modelling of water waves. In: *Phys. Modelling in Coastal Eng.* (Eds. Dalrymple, R.A., E. Balkema, A.A. Rotterdam). The Netherlands, 13-47

Traykovski, P., Hay, A.,H., Irish, J.D. and Lynch, J.F. 1999. Geometry, migration, and evolution of wave orbital ripples at LEO-15. *J. Geophys. Res.,* 104(C1), 1505-1524.

Vittory, G. and Blondeaux, P. 1990. Sand ripples under sea waves. Part 2. Finite-amplitude development. *J. Fluid Mech.*, **218**, 19-39.

Voropayev, S.I., Cense, A. W., McEachern, G.B., Boyer, D.L. and Fernando, H.J.S. 2001, Dynamics of cobbles in the shoaling region of a surf zone. *Ocean Eng.,* 28, 763-788.

Voropayev, S.I., McEachern, G.B., Boyer, D.L. and Fernando, H.J.S. 1999. Dynamics of sand ripples and burial/scouring of cobbles in oscillatory flow. *Applied Ocean Res.*, **21**(5), 249-261.

Voropayev S.I., McEachern G.B., Boyer D.L. and Fernando, H.J.S. 2000. Drifting sand ripples and burial of cobbles in near-shore zones. *Oceanic Fronts and Related Phenomena* Intergovernmental Oceanographic Commission, Workshop Report No 159, UNESCO'99., 167-172.

Voropayev, S.I., Roney, J., Fernando, H.J.S., Boyer, D.L. and Houston W.N. .1998. The motion of large bottom particles (cobbles) in a wave-induced oscillatory flow. *Coastal Eng.,* **34**, 197-219.

Voropayev S.I., Testik F.Y., Boyer D.L. and Fernando H.J.S. 2003. Morphodynamics and cobbles behavior in and near the surf zone. *Ocean Engr.*, in press

Whitham, G.B. 1955. The effects of hydraulic resistance in the dam-break problem. *Proc. Royal Soc.*, Ser. A, **227**, 399-407.

Whitham, G.B. 1974. *Linear and Nonlinear Waves.* John Wiley & Sons, New York.

Yalin, M.S. 1977. *Mechanics of Sea Bed Transport.* Pergamon, New York.

Yu, J. and Mei, C. C. 2000. Formation of sand bars under water waves. *J Fluid Mech.,* **416**, 315-348.

8. Publications

Luccio P.A., Voropayev S.I., Fernando H.J.S, Boyer D.L and Houston W.N. 1998. Motion of cobbles in the swash zone on an impermeable slope. *Coastal Engineering.*, 33, 41-60.

Voropayev S.I., Cense A.W., McEachern G.B. 1999. Cobble dynamics in the wave-breaking region along an impermeable slope In: *Abstracts of Fifteenth Arizona Fluid Mechanics Conference,* Tucson, Arizona, April 23-24, 1999, 2-3.

Voropayev S.I., Cense, A.W., McEachern G.B., Boyer, D.L. and Fernando, H.J.S. 2001. Dynamics of cobbles in the shoaling region of a surf zone. *Ocean Engineering*, 28(7), 763-788.

Voropayev S.I., Cremers M.F.G., Boyer D.L. and Fernando H.J.S. 2001. Dynamics of burial of cobbles/mines in the coastal zone. *Oceanography*, **14**(1), 55-56.

Voropayev S.I., McEachern G.B., Boyer D.L. and Fernando, H.J.S. 2000. Drifting sand ripples and burial of cobbles in near-shore zones. *Oceanic Fronts and Related Phenomena* Intergovernmental Oceanographic Commission, Workshop Report No 159, UNESCO'99, 167-172

Voropayev, S.I., McEachern, G.B., Boyer, D.L. and Fernando, H.J.S. 1999. Dynamics of sand ripples and burial/scouring of cobbles in oscillatory flow. *Applied Ocean Research.*, **21**(5), 249-261.

Voropayev S.I., McEachern G.B., Boyer D.L., Fernando H.J.S. 2000. Drifting sand ripples and burial of cobbles in near-shore zones. *Oceanic Fronts and Related Phenomena,* Intergovernmental Oceanographic Commission, Workshop Report No 159, UNESCO, 574-579.

Voropayev S.I., Roney J., Fernando H.J.S., Boyer D.L. and Houston W.N. 1998. The motion of large bottom particles (cobbles) in a wave-induced oscillatory flow. *Coastal Engineering,* **34**, 197-219.

Voropayev S.I., Testik F.Y., Boyer D.L. and Fernando H.J.S. 2001. Migrating ripples and burial of cobbles/mines in a coastal zone *Proceedings of the 2001 International Symposium on Environmental Hydraulics, December 2001, Tempe, USA.*

Voropayev S.I., Testik F.Y., Boyer D.L. and Fernando H.J.S. 2003. Morphodynamics and cobbles behavior in and near the surf zone. *Ocean Engineering*, in press

Voropayev S.I., Testik F.Y., Boyer D.Land Fernando H.J.S. 2002. Morphodynamics and burial/scouring of cobbles in a coastal zone. *EOS, Transactions, American Geophysical Union*, 83(4), OS56-OS57.